Scattering Effect on Optical Performance of Quantum Dot White Light-Emitting Diodes Incorporating SiO$_2$ Nanoparticles

Zong-Tao Li, *Member, IEEE*, Jie-Xin Li, Jia-Sheng Li, Zi-Hao Deng, Yue-Hua Deng, and Yong Tang

Abstract—The scattering effect plays an important role in improving the optical performance of the quantum dot (QD) white light-emitting diodes (LEDs). A majority of the previous studies have focused on the planar packaging structure only with respect to total internal reflection (TIR). In this study, SiO$_2$ nanoparticles are incorporated into QD-silicone encapsulation of LEDs with semi-spherical lens packaging (SSLP) to exploit their scattering effect. The results show that the radiant efficacy (31.35%@100 mA) and luminous efficacy (87.56 lm/W@100 mA) of QD white LEDs can be optimized using SiO$_2$ nanoparticle concentration (0.1 wt%) and that they increase by 5.04% and 11.08%, respectively, as compared to the conventional structure. A comprehensive ray-tracing simulation validates that the nanoparticles in the SSLP structure lead to severe loss of chip light. On the contrary, the fluorescence light increases due to the enhancement of conversion by QDs. The transmission electron microscopy images and the finite-difference time-domain simulation have been introduced to investigate the surface adsorption of SiO$_2$ nanoparticle. This study indicates that SiO$_2$ incorporation is an effective method to improve the efficiency of QD white LEDs, and provides a better understanding on the scattering effect based on TIR, color conversion, and surface adsorption.

Index Terms—Quantum dot white LED, scattering, SiO$_2$ nanoparticles, semi-spherical lens packaging structure.

I. Introduction

LIGHT-EMITTING diodes (LEDs) are widely used as solid-state light sources owing to their lower cost, longer life, higher efficiency, and environmental sustainability [1]–[4]. The most basic and commonly used method for developing white LEDs is combining blue LEDs chip [5], [6] with down-conversion phosphor along with rare-earth-based YAG and nitride phosphor [7]–[9]. Thus far, several attempts have been made to improve the efficiency and stability of phosphor-converted LEDs [10]–[13]. However, it is extremely difficult to meet the future demand for wide color gamut due to natural limitations of phosphoric materials such as low color purity [7]. In recent years, the quantum dot (QD) has gained popularity as LED packaging owing to their improved cost efficiency, high quantum yield, and size-dependent emission color, as compared to traditional luminescent materials [14], [15]. In particular, QDs have a narrow and symmetric full-width at half maximum which is less than 20 nm, indicating that the color of the emission light is purer than that of the conventional rare-earth based phosphor. This plays a vital role in display based applications that require high color purity [16]. Furthermore, QDs are widely used in applications such as solar cells, biomarkers, chemical catalysts, sensors, and photoelectric devices [17]–[19]. Recently, they have been considered as potential color converting materials that can be used for display and illumination- based applications [14], [20]–[22].

The QD white LED has gained immense popularity in the field of research due to the advantages of photoluminescent QDs [23], [24]. Industrial production of QD white LEDs is highly challenging. One of the major challenge is that the efficiency [25] of current QD white LED is lesser than that of matured phosphor-converted LEDs [26]. Several methods have been studied to address the issues pertaining to white LED technology. The previous studies on phosphor-converted LEDs indicate that their efficiency can be increased by incorporating different nanoparticles in the silicone encapsulant [27]. Chen *et al.* [28] proved that the luminous efficacy of a white LED with the remote ZrO$_2$-incorporated phosphor structure increased by 2.25% due to the refractive-index gradient created by ZrO$_2$ nanoparticles. Zheng *et al.* [29] added a TiO$_2$/silicone encapsulation layer to the bottom of chip-on-board packaging LEDs to redirect the backscattering blue light to extract the encapsulation materials. It was found that the extraction of light decreased with increase in the concentration of phosphor which indicated that the original scattering ability of phosphor restrains the light-extraction ability of the nanoparticles. Thus, it can be inferred that light-extraction of QD-converted LED can be increased by inducing nanoparticles which weakens the scattering ability of QDs [30]. In our previous study [16], we incorporated ZnO nanoparticles into QD white LEDs and
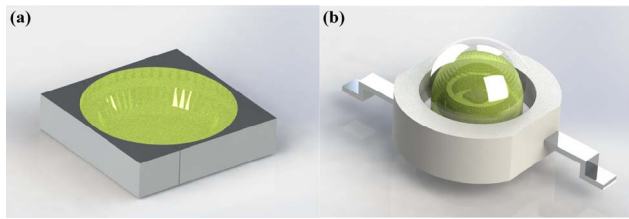
Fig. 1. (a) Diagram of the LED with planar packaging (PP) structure. (b) Diagram of the LED with semi-spherical lens packaging (SSLP) structure.
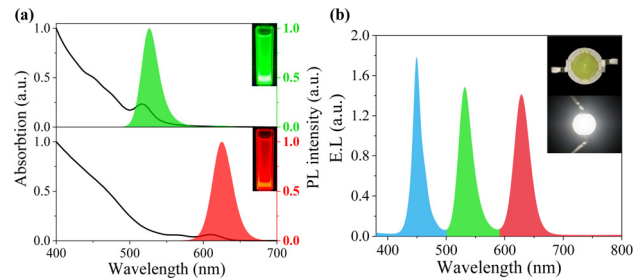

Fig. 2. (a) Absorption and PL spectra of green and red CdSe/ZnS QDs solution, and the inserts show the green and red QDs solution. (b) The spectrum of QD white LEDs. The insert shows the images of LEDs using SSLP structure under the injection current of 0 mA (top) and 100 mA (bottom).

found that the luminous flux increased by 3.37% as compared to the conventional structure with same output color.

A majority of the previous studies incorporating nanoparticles have focused on the planar packaging (PP) structure and have not considered the semi-spherical lens packaging (SSLP) structure. Regarding the enhancement mechanism in the PP structure, nanoparticles significantly reduce the loss due to total internal reflection (TIR) by changing the direction of propagation of the TIR light [8]. The SSLP structure has an advantage over PP structure due to higher light-extraction and negligible TIR loss; however, there is no literature referring to the incorporation of nanoparticles in SSLP structures.

In this study, different amounts of SiO_2 nanoparticles are uniformly incorporated into the silicone encapsulation of QD white LED with SSLP structure. First, SiO_2-only films are fabricated to confirm the scattering ability of SiO_2 nanoparticles, and the impact of different concentration of SiO_2 on radiant efficacy, luminous efficacy and corelated color temperature (CCT) is determined experimentally. Subsequently, a comprehensive simulation is conducted to obtain a deeper understanding of the scattering effect. Additionally, a few discussions have been included to explain the enhanced optical efficiency caused by the surface adsorption of SiO_2 nanoparticles.

II. EXPERIMENTAL

Fig. 2(a) represents the photoluminescence (PL) spectra under 365-nm light excitation and absorption spectra of green and red CdSe/ZnS QDs solution purchased from Beijing Beidajubang Science & Technology Co., Ltd, which is tested by fluorospectro photometer. It can be observed that green QDs have an absorption edge of ~520 nm and their emission peak wavelength is ~525 nm. Similarly, the red QDs have an absorption edge of ~620 nm and their emission peak wavelength is ~625 nm. The QD white LEDs are developed using the following procedure. Firstly, 3.5 mg CdSe QD powder (mass ratio of green QD to red QD is 19:1) is completely dissolved into 3 ml of chloroform and mixed with 1 g polydimethylsiloxane (PDMS) purchased from Dow Corning Co., Ltd. Subsequently, the chloroform-silicone-QDs mixture is evaporated at 50 °C to volatize the chloroform completely and to obtain the QD-slurry. Next, the QD-slurry is mixed with varying amount of SiO_2 nanoparticles based on the concentration of the SiO_2 to obtain the QD-SiO_2-slurry. This is followed by fabrication of QD white LEDs. LEDs with SSLP structure have been selected to conduct the study. The polycarbonate lens is 5.6 mm in diameter and its thickness is 0.6 mm. The blue LED chip has a horizontal structure

with the dimensions 1.143 mm × 1.143 mm × 0.1 mm, and its wavelength is centered at 455 nm. The prepared slurry is injected into the lens to fill the gap and is measured to be 37 mg in devices. Finally, these devices are moved to the oven set at 60 °C for 2 h to cure the silicone. The optical performances are measured using an integrating sphere system. As seen in Fig. 2(b), the spectra of QD white LEDs is measured under an injection current of 100 mA. It is observed that three emission peaks originate from the chip, namely, green and red QDs. The blue, green and red lights are combined to produce white color for wide-color-gamut display. The insert shows the images of LEDs with SSLP structure under the injection current of 0 mA (upper) and 100 mA (lower).

To study the impact of scattering of SiO_2 nanoparticles (purchased from Aladdin, mean particle size of 250 nm), different SiO_2 nanoparticles-only films are fabricated with their concentration varying from 0 to 2 wt%. The process of manufacturing is similar to that of QD-SiO_2-slurry. Firstly, varying amounts of SiO_2 nanoparticles are doped uniformly with 1 g PDMS based on the concentration of SiO_2. Subsequently, the mixture is injected into a stainless-steel mold and moved to the oven set at a temperature of 120 °C for 1 h to cure the silicone. Finally, the SiO_2-only films are obtained with a thickness of 2 mm which helped in studying the scattering ability of SiO_2 nanoparticles. The transmittance and haze spectra of these films are measured using a fluorescence spectrometer. Fig. 3(a) depicts the transmittance spectra. It is observed that the transmittance of the film decreases with increase in the concentration of SiO_2 nanoparticles due to reverse scattering. Fig. 3(b) depicts the haze spectra of different SiO_2 concentrations. It is observed that the haze increases with increase in the concentration of SiO_2. The haze of the film increases from 6.9% to 67.6% at a typical wavelength of 450 nm as the concentration of SiO_2 increased from 0% to 2%. Therefore, it can be confirmed that SiO_2 nanoparticles enhance the scattering ability, and it increases with the increase in the concentration of SiO_2. The haze of SiO_2-only film increases and its transmittance increases with increase in the concentration of SiO_2. Thus, SiO_2 nanoparticles have a remarkable impact on the light emitted from chips, such as blue light, as compared to the fluorescence generated by QDs. The particle size of SiO_2 nanoparticles is larger as compared to the blue wavelength; thus, they exhibit a stronger scattering effect.
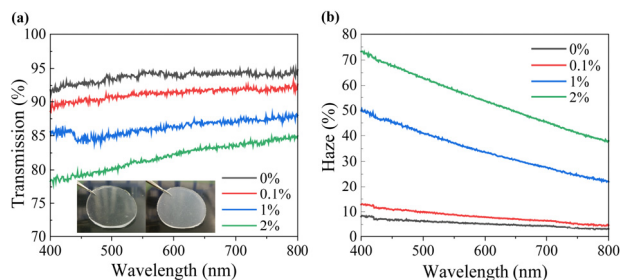
Fig. 3. Transmissivity (a) and haze (b) of SiO$_2$-only films with different concentrations. The insert shows the images of SiO$_2$-only films with SiO$_2$ concentration of 0 wt% (left) and 1 wt% (right).
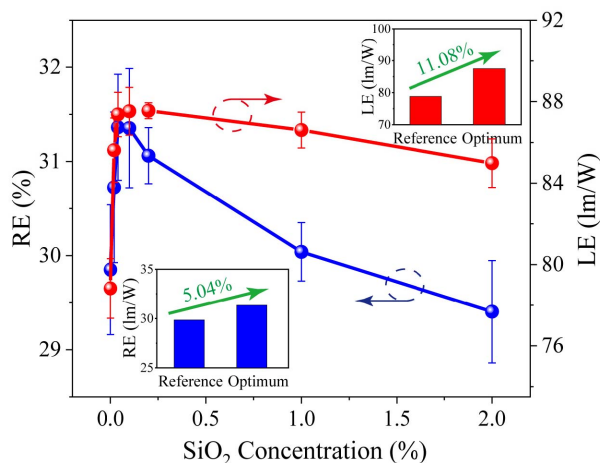

Fig. 4. Radiant efficacy (RE) and luminous efficacy (LE) of QD white LEDs with different concentrations of SiO$_2$ nanoparticles under the injection current of 100 mA. The inserts show the improvement in RE and LE.

Fig. 5. Color proportion (a) and peak intensity (b) of the QD white LEDs with different concentrations of SiO$_2$ nanoparticles under the injection current of 100 mA.

III. RESULTS AND DISCUSSION

The QD white LEDs, incorporated with different concentrations of SiO$_2$ nanoparticles, are prepared and their optical performance is investigated to study the impact of SiO$_2$ nanoparticles. Fig. 4(a) depicts the radiant efficacy (RE) which increases initially and eventually reaches its maximum value at 0.1 wt% concentration. The SiO$_2$ nanoparticles increase the RE by 5.04% as compared to the conventional QD white LEDs without incorporation of SiO$_2$. Most previous studies indicate that the RE increases due to reduction in TIR loss of the light emitted from chips in PP structure [31]. It is noticeable that almost no TIR loss is seen in SSLP structure and the explanation for the same will be discussed later. Fig. 4(b) depicts the luminous efficacy (LE) of the QD white LEDs using varying concentrations of SiO$_2$ nanoparticles. It is observed that the LE increases rapidly at initial stage due to an increase in the concentration of SiO$_2$. However, the LE slowly decreases as the concentration reaches the optimum level. The LE of QD white LED optimized with SiO$_2$ nanoparticle is found to be 11.05% higher than the conventional QD white LEDs without SiO$_2$, reaching high LE of 87.56 lm/W @100 mA.

The impact of SiO$_2$ nanoparticles on QD white LED may not be completely identical to that on conventional phosphor-convert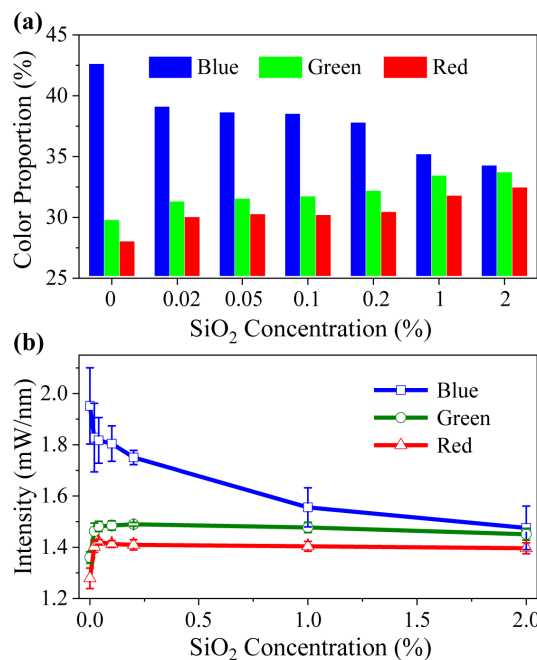ed LEDs. Spectra energy analysis is conducted to gain a deeper understanding of the scattering effect. The blue-light radiant power from 380–480 nm, green-light radiant power from 480–540 nm and red-light radiant power from 540–780 nm are individually extracted by integrating the corresponding energy of the spectra. Fig. 5(a) depicts the color proportion of the QD white LED with different concentrations of SiO$_2$ nanoparticles. It is observed that the proportion of blue light monotonically decreases whereas that of green and red light increases with an increase in the concentration of SiO$_2$. Similarly, the peak intensity of blue light decreases, whereas that of green and red light increase with the concentration, as seen in Fig. 5(b). This variation in intensity is attributed to the higher concentration of SiO$_2$ nanoparticles, which enhances the scattering effect. As the scattered blue light traverses complex optical paths in encapsulation materials, additional blue light is absorbed by QDs. Moreover, excessive SiO$_2$ nanoparticles increase the backscattering of blue light; thus, additional blue light is absorbed by the substrate. In contrast, the green and red light increase initially due to the enhanced conversion of QD, which can be attributed to the additional absorption of blue light by QDs. The intensity of green and red lights get saturated as the concentration continues to increase. Thus, the scattering effect can also increase the optical path of lights excited from QDs, thereby increasing the inter-absorption and reabsorption loss between QDs [32].

The chromaticity coordinates of the QD white LED with varying concentration of SiO$_2$ nanoparticles is shown in Fig. 6. The chromaticity coordinates gradually move toward the yellow region as the concentration increases. This phenomenon is attributed to the aforementioned spectra energy analysis, reduction of blue light, and improvement in color conversion due to stronger scattering effect. Correspondingly, the CCT
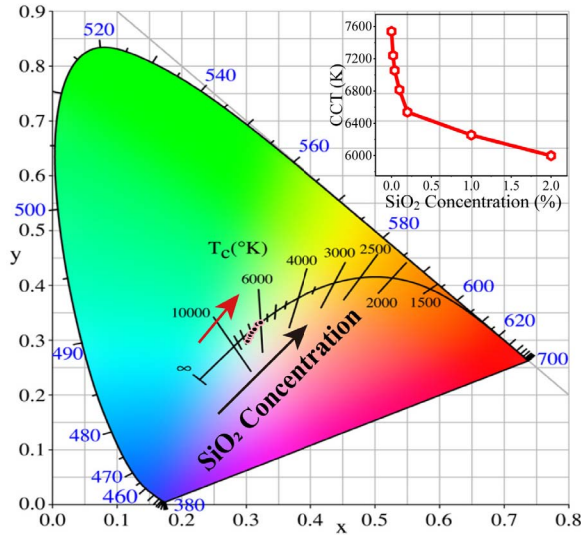
Fig. 6. CIE 1931 chromaticity coordinates of QD white LEDs with different concentrations of SiO_2 nanoparticles. The insert presents their CCT with different concentrations of SiO_2 nanoparticles.

decreases from 7539 K to 5999 K as the concentration increases from 0 to 2%, as seen in the insert. This phenomenon indicates that the incorporation of SiO_2 prevents the usage of QDs for reducing CCT [33].

For a deeper understanding of the scattering effect, a comprehensive simulation was conducted using the ray-tracing model in the commercial software TracePro. The impact on the light emitted from chips and QDs are analyzed to determine the scattering mechanisms. A systematic simulation that is not limited to the SiO_2 particles was introduced. Moreover, a scattering distribution function was implemented in TracePro to study the scattering effect, and it is defined as follows [34]:

$$SDF = p(\theta) = \frac{1 - g^2}{4\pi (1 + g^2 - 2g\cos\theta)^{3/2}}$$

where g is the anisotropy factor, that represents the scattered energy distributions and depends on the structure of nanoparticles.

When a ray enters the scattering medium, it propagates for a random distance x, governed by the following probability distribution:

$$P(x) = e^{-\mu x} dx$$

where μ is the scattering coefficient that represents the scattering probability and depends on the concentration of nanoparticles.

A loss in optical energy is observed in the case of substrates with specific absorbance to visible light. Therefore, the reflectivity of the substrate R (from 0 to 1) is considered as a parameter to develop the simulations comprehensively. The simulations that focus on the lights emitted from chips only, are conducted and the radiant power of the output light (PC_{opt}) is recorded. Fig. 7(a) depicts the output light emitted by the chips which decreases monotonously with an increase in the concentration of nanoparticles when the reflectivity is varied

from 0 to 0.98. The output lights under different reflectivities are observed to be identical initially. However, discrepancy arises when the concentration of nanoparticles reaches its optimum value. Higher reflectivity leads to emission of more output lights from chips due to lesser absorption of lights by the substrate. Fig. 7(b) depicts the impact of different nanoparticles. Lesser output lights are observed while using the nanoparticles with lower g. Generally, a lower g factor indicates that the nanoparticles have a strong back-scattering ability. Nanoparticles with strong backscattering ability emit more light from chips absorbed by QDs and substrates. The absorption of light by QDs (PC_{abs}) has also been studied along with the output lights as seen in Fig. 7(c). The absorption by QDs increases with increase in the concentration and reflectivity. The light emitted from the chips has a longer optical path and higher possibility of conversion owing to the scattering effect of nanoparticles. It is observed that absorption decreases rapidly as the scattering coefficient μ increases. In other words, the inordinate nanoparticles lead to lesser conversions. The nanoparticles form a barrier with extremely strong backscattering ability around the chip, and most of the lights emitted from the chip can be trapped immediately and back scattered to the substrate. Thus, the possibility of conversion decreases sharply and the absorption by QDs is reduced.

Fig. 7(d) depicts the absorption by QDs with different types of nanoparticles. As shown in the figure, a variety of nanoparticles affect the value of the absorption peak. The nanoparticles with high backscattering ability initially increase the absorption at a faster rate and attain the peak value earlier than expected. As a high backscattering effect increases the optical path of light emitted from the chips and increases the possibility of absorption by QDs, the absorption is faster. The maximum absorption by QDs is observed at a high value of the g factor, which confirms that strong backscattering does not improve the possibility of color conversion, as presented in Fig. 7(c). Therefore, it is suggested that particles with weak backscattering ability may be selected for enhancing color conversion events.

On the basis of the abovementioned analysis, the light emitted from the chips are categorized as the output light, the light absorbed by QDs, and the light absorbed by substrate. However, only the output light and the light absorbed by QDs helps in increasing the overall efficiency of the devices. Therefore, the sum of the output light and the absorption by QDs ($PC_{opt+abs}$) has been introduced to study the loss of optical energy caused by the substrate. Fig. 7(e) and (f) depict the $PC_{opt+abs}$ with different reflectivity and g factor, respectively. The $PC_{opt+abs}$ decreases continuously with increase in the scattering coefficient, i.e., the loss due to the substrate increases. It is observed that $PC_{opt+abs}$ decreases rapidly in case of substrate with lower reflectivity or the nanoparticles with high backscattering ability (lower g). This phenomenon indicates that the nanoparticles enhance the conversion by QDs and increase the loss of optical energy by the substrate.

The experiment on SiO_2-only LEDs was conducted to validate the simulation results. Devices with varying concentration of SiO_2 nanoparticles were developed, and their optical
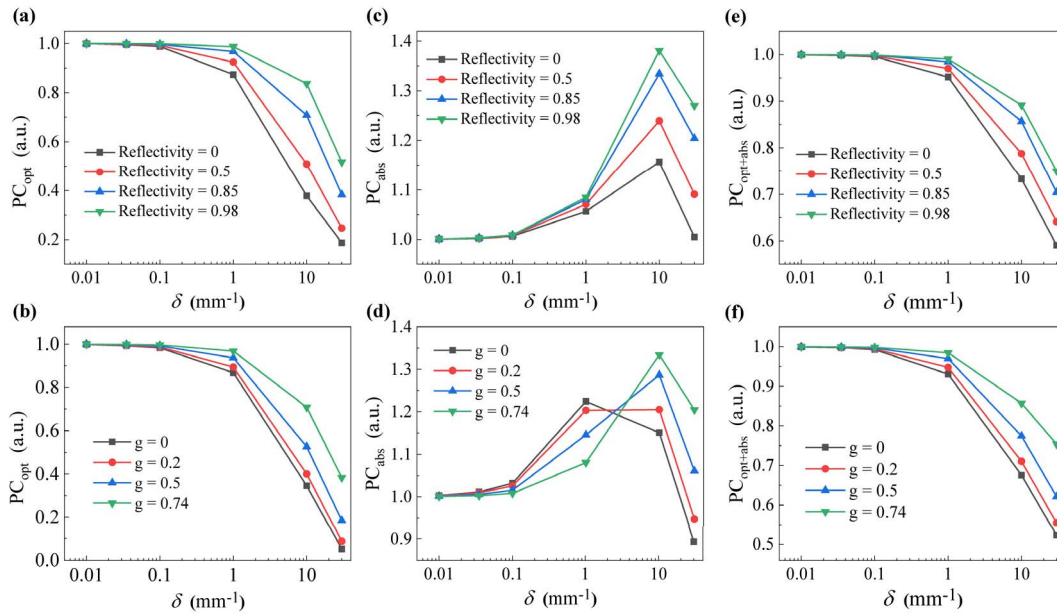
Fig. 7. (a-b) Normalized output light (c-d) Normalized light absorption by QDs (e-f) Normalized sum of the output light and the absorption by QDs when considering only the lights emitted from chips.
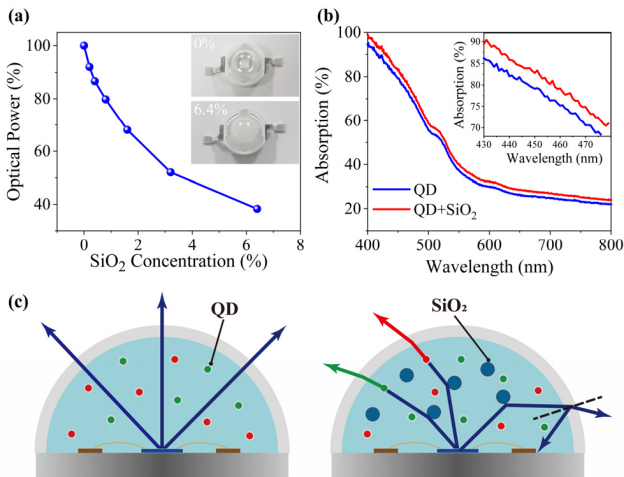

Fig. 8. (a) Optical power of blue light of SiO₂-only LEDs with different concentrations of SiO₂ nanoparticles. The inserts show the images of SiO₂-only LEDs with SiO₂ concentration of 0% (top) and 6.4% (bottom). (b) The absorption difference between QD film without and with SiO₂ nanoparticles. (c) Dynamic analysis of rays in QD white LED with and without SiO₂ nanoparticles only considering the light emitted from chip.

performances are investigated, as shown in Fig. 8(a). It is observed that the optical power decreases monotonously with an increase in the concentration, similar to the result of the simulations. This phenomenon confirms that the output light emitted from the chip is reduced due to the backscattering effect caused by SiO₂ nanoparticles. Fig. 8(b) depicts the difference in absorption by the QD film and the QD film incorporated with SiO₂ nanoparticles, with identical thicknesses and concentrations. It is observed that the SiO₂ nanoparticles increase the rate of absorption, as compared to the conventional film. From the insert, it is evident that the QD film

incorporated with SiO₂ nanoparticles exhibits higher absorption at a wavelength of 455 nm. Thus, SiO₂ nanoparticles play an important role in enhancing the absorption of lights emitted from chip by QDs. Fig. 8(c) represents the schematic illustration of the light output mechanism from chip with SiO₂ nanoparticles and the chip without SiO₂ nanoparticles. The blue light emitted from the chip escapes from the conventional QD white LEDs owing to the weak TIR in SSLP structures and the weaker scattering of QDs. Thus, the blue light is not fully utilized for the conversion by the QDs. However, this scattering ability is significantly enhanced by incorporating SiO₂ nanoparticles, and the blue light exhibits longer optical paths in the encapsulation materials and a high possibility of conversion by QDs. The loss of substrate deteriorates drastically, as observed during the simulations. The SiO₂ nanoparticles change the direction of emission of the blue light with a larger incident angles at the interface between the lens and the free region, thereby generating additional Fresnel reflection and TIR loss in the devices [35].

The effect of scattering on the output fluorescence light is investigated through simulations. In this case, the amount of fluorescence light converted by QDs is treated as constant and the scattering-dependent absorption of blue light is neglected. As illustrated in Fig. 9(a), the power of output fluorescence light (PF_{opt}) with different reflectivities decreases with increase in the concentrations of nanoparticles. Substrate with higher reflectivity leads to a gradual decrease in the power of output fluorescence light (PF_{opt}) owing to lesser loss by the substrate as seen in the output blue light from chip. Fig. 9(b) depicts the impact on output fluorescence light using different nanoparticles with different g factor. Nanoparticles with higher backscattering ability result in a rapid decrease. Therefore, it is suggested that the output fluorescence light reduces when the devices are doped with nanoparticles. The nanoparticles
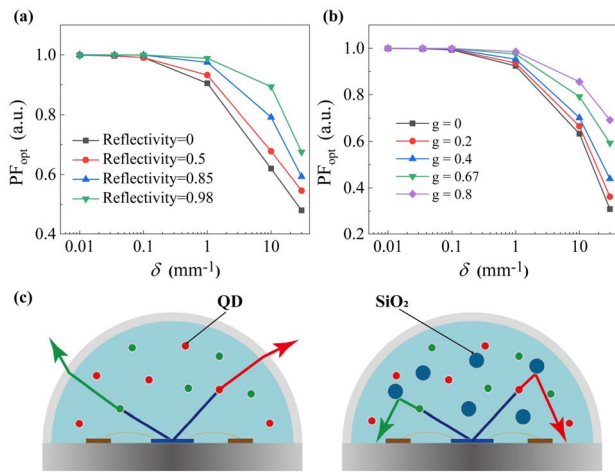
Fig. 9. (a) The normalized power of output fluorescence light (PF_{opt}) with different reflectivities. (b) The normalized power of output fluorescence light (PF_{opt}) with different g factors. (c) Dynamic analysis of rays in QD white LED with and without SiO_2 nanoparticles only considering the QD light.
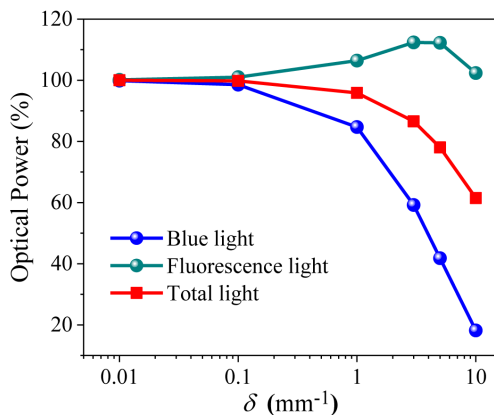

Fig. 10. Optical power of blue, fluorescence and total light (the sum of optical power of blue light and fluorescence light).

increase the possibility of absorption of fluorescence light by substrate, thereby reducing the PF_{opt}, as seen in Fig. 9(c).

To investigate the comprehensive impact of nanoparticles on the structure of SSLP, both the blue light emitted from chip and the fluorescence light emitted from QDs are taken into consideration. The optical power of blue light, fluorescence light and total light (the sum of optical power of blue light and fluorescence light) is depicted in Fig. 10. It is observed that the blue light decreases monotonously with increase in the concentration of the nanoparticles. However, the fluorescence light increases initially and reaches its peak value which is contrary to the results of the simulation. The scattering effect increases the probability of absorption of chip light by QDs and enhances the conversion events, thereby strengthening the optical power of the fluorescence light as discussed in Fig. 7. The optical power of the fluorescence light reduces as the concentration of nanoparticles increases owing to the heavy back-scattered loss as discussed in Fig. 9. It is important to mention that the optical power of total light decreases with increase in the concentration. These results show that the

nanoparticles in SSLP structure are responsible for severe loss of optical energy in chip light and for increasing the optical power of fluorescence light at lower concentration of SiO_2 incorporation, which is attributed to the enhancement of conversion events from QDs.

A series of simulations are conducted to demonstrate that the conventional method of incorporating nanoparticles is not sufficient for increasing the total optical power in SSLP structure while considering the backscattering effect of the encapsulant. Experiment on QD white LEDs shows that SiO_2 nanoparticles increase in RE by 5% as compared to the conventional devices (Fig. 4). Previous studies indicate that SiO_2 particles can be used as an adsorbent owing to their porous surface [36], and the QDs are adsorbed onto the SiO_2 particles during the process of packaging. For better understanding, the transmission electron microscopy (TEM) images of SiO_2 nanoparticles and QD/SiO_2 hybrid particles are illustrated in Fig. 11 (a). It is stated that the hybrid particles are obtained by wet mixing with a solvent. The solvent used in experiments is chloroform and silicone is not added for convenient measurement of TEM. In the upper picture of Fig. 11(a), it is observed that the SiO_2 nanoparticles without QDs have a spherical geometry, and they appear white in color under sunlight and ultra-violet (UV) light. In contrast, the lower picture of Fig. 11(a) shows that the QD/SiO_2 hybrid particles appear in a uniform green color under UV light. TEM image depicts that the spherical QDs are located on the surface of SiO_2 nanoparticles. The noticeable difference between these two TEM images indicates that SiO_2 nanoparticles have a strong ability for surface adsorption in respect to QDs as reported by previous studies [37], [38]. The simulations of the ray-tracing model are carried out on the basis of the assumption that the QDs and SiO_2 nanoparticles are uniformly dispersed in the encapsulation materials without any interaction. In order to investigate the impact of their interaction on optical performance, a three-dimensional finite-difference time-domain (FDTD) model has been built, which is developed as a commercial software by Lumerical FDTD Solution. During the simulations, the FDTD method is used to solve the Maxwell's curl equation based on the Yee cell [39]. The cross-sectional view for with and without SiO_2 nanoparticles is illustrated in Fig. 11(b). It is observed that the QDs are located around the SiO_2 nanoparticles. The perfectly matched layer is used as the boundary condition, which surrounds the FDTD calculation region for absorbing the escaping light. Electromagnetic field detectors are used to record the electromagnetic energy distributions of the propagating light. A dipole source with isotropic emission is considered to be the QD light source, and the down-conversion processes are not taken into consideration [40], [41]. Silicone is used as the background material for the free region. For successive simulations the complex refractive index of SiO_2 nanoparticles and CdSe/ZnS QDs are set as per the literatures [42], [43].

According to the TEM images shown in Fig. 11(a), the QDs are set with diameters of 10 nm. The number of QDs are selected on the basis of the concentration of SiO_2 nanoparticles and they are distributed uniformly on the surface of SiO_2 nanoparticles. Optimum mesh size is calculated to be 0.05 nm
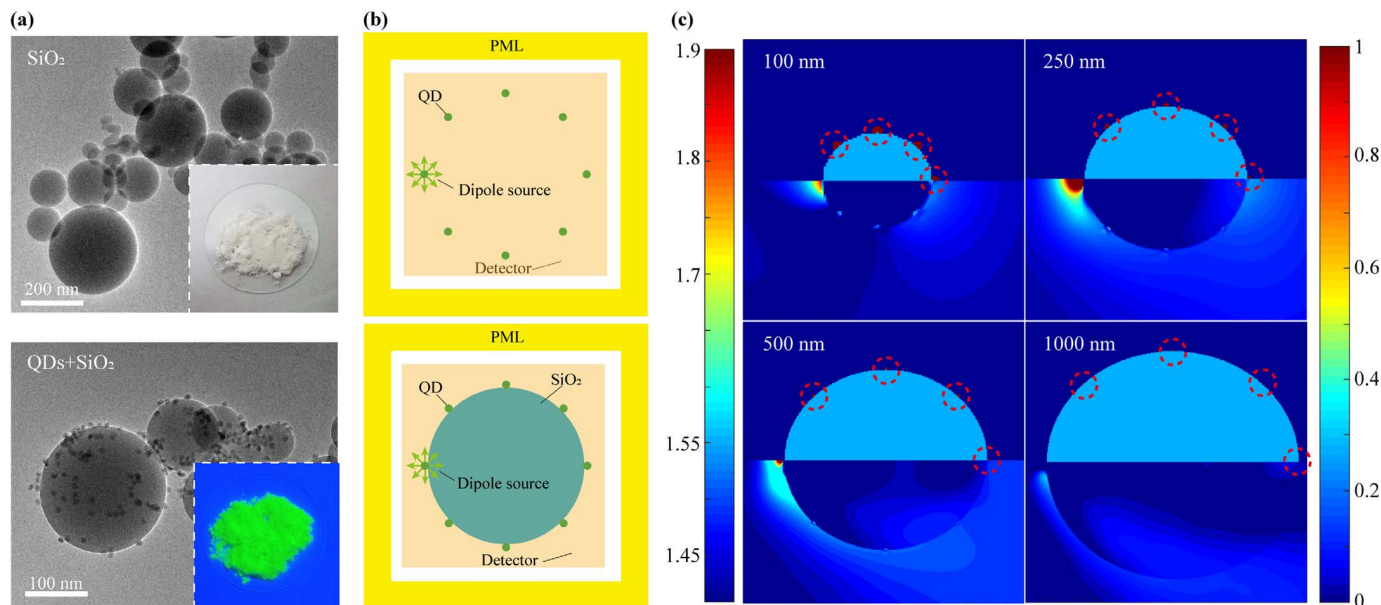
Fig. 11. (a) TEM images of SiO₂ nanoparticles without QDs (top) and with QDs (bottom). The inserts show the SiO₂ powder with and without QDs. (b) The cross-section view of the three-dimensional finite-difference time-domain (FDTD) model. QD model (top) and SiO₂/QD model (bottom). (c) Refractive index distributions (top) and difference distributions in electromagnetic field (bottom) using SiO₂ nanoparticles with diameter of 100, 250, 500, 1000 nm. The left color bar is related to the refractive index distributions and the right color bar is related to the difference distributions. The dotted line red circles are emphasized to show the positions of QDs.

which ensure the accuracy of the simulation and the simulation time is set to ensure convergence of energy.

Fig. 11(c) depicts the refractive index distributions and difference in electromagnetic field when the SiO₂ nanoparticles are set with diameter of 100, 250, 500, 1000 nm, respectively. Owing to the distributions of refractive index and electromagnetic field are symmetrical, they are combined to intuitively show the impacts caused by SiO₂ nanoparticles with different sizes. The refractive index distributions show the SiO₂/QD models with different sizes and the positions of QDs are also emphasized for convenient observation. The difference in electromagnetic field was computed using $P = P_{SiO2/QD} - P_{QD}$, where, $P_{SiO2/QD}$ is the intensity of SiO₂/QD model, and P_{QD} is the intensity of QD model. The normalized intensity depicts the field of optical enhancement and it is observed that most of the region, where the optical power is enhanced (larger than zero), are distributed on the region of QD light source. Obviously, the optical power is also enhanced in the regions of QDs, meaning that most of the light propagate around the SiO₂ nanoparticle. Furthermore, it can be observed that more light propagates through the SiO₂ nanoparticle with the increase of diameter, thereby enhancing the optical power. Particularly, the optical enhancements in the region of QDs are retained when the SiO₂ nanoparticles are set with different size. This indicates that the SiO₂ nanoparticle cause near-field scattering effect of light, increasing the probability of being captured by QDs around the SiO₂ nanoparticles. Therefore, the results show that the interaction leads to more light trapped in QDs and deteriorative reabsorption no matter what the size of SiO₂ nanoparticles is.

Recently, previous studies indicate that the aggregation of QDs in polymer matrix reduces the color conversion efficiency
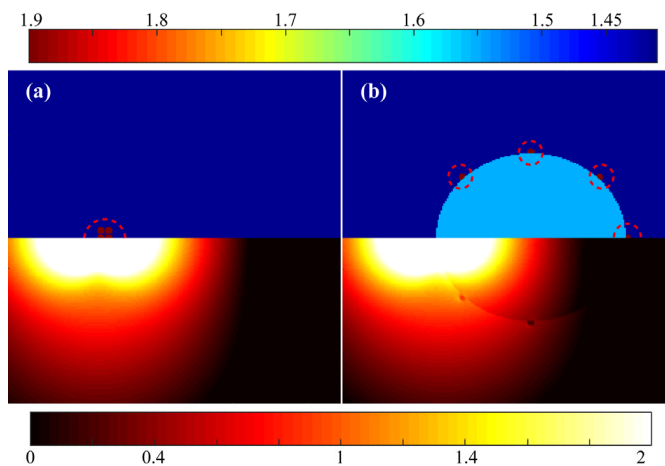

Fig. 12. Refractive index distributions (top) and electromagnetic field distributions (bottom) of (a) aggregative QDs model and (b) SiO₂/QD interaction models. The top color bar is related to the refractive index distributions and the bottom color bar is related to the electromagnetic field distributions. The dotted line red circles are emphasized to show the positions of QDs.

of QD white LEDs and it is an efficient method to improve the dispersion of QDs through the nanopores designs, largely enhancing the optical power of devices [43]. This means that the QDs are probably aggregative instead of uniformly dispersing in the encapsulation materials and the adsorption of QDs by silica prevents aggregation. Furthermore, the aggregative QDs model and SiO₂/QD interaction models were also built up to investigate the impact caused by SiO₂ nanoparticles. As shown in Fig. 12(a), it is noticeable that the aggregative QDs are almost concentrated in the center of QD source,

meaning that the aggregation leads to more serious reabsorption of QDs. However, the QDs are distributed at the SiO_2 surface shown in Fig. 12(b), where the radiant energy is much smaller than that of QD source region. This is attributed to the fact that the interaction of SiO_2 nanoparticles largely improve the dispersion of QDs, reducing the probability of being captured by aggregative QDs. Therefore, enhanced RE and LE can also be attributed to strong surface adsorption of SiO_2 nanoparticles. Additionally, it is important to investigate the effect of adsorption on QDs in a more comprehensive and micro perspective manner.

IV. Conclusion

In this study, we investigated the scattering effect on the QD white LEDs with SSLP structure using SiO_2 nanoparticles. The scattering ability due to SiO_2 nanoparticles is proved by a series of SiO_2 nanoparticle-only films. The results show that the RE (31.35%@100 mA) and luminous efficacy (87.56 lm/W@100 mA) of QD white LEDs can be optimized using SiO_2 nanoparticle concentration (0.1 wt%) and they increase by 5.04% and 11.08%, respectively, as compared to the conventional structure. The spectra energy analysis reveals that these results are attributed to enhanced utilization of blue light, thereby increasing the conversion of QDs. As a result, the chromaticity coordinates moved to the yellow region as the concentration increases. For deeper understanding of the scattering effect, a comprehensive simulation is conducted using the ray-tracing model. It is observed that the nanoparticles in the SSLP structure lead to severe loss of chip light. On the contrary, the fluorescence light increases due to the enhancement of conversion by QDs. The overall efficiency is reduced owing to higher TIR loss and back-scattered loss by nanoparticles in case of scattering effect only. For better understanding on this, TEM images and FDTD simulations are investigated. The results show that SiO_2 nanoparticles have a strong adsorption ability for QDs, which probably helps to suppress the aggregation and light reabsorption between QDs. Consequently, this study provides an effective method to enhance the optical efficiency for QD white LEDs with SSLP structure by incorporating SiO_2 nanoparticles. Furthermore, it also provides a better understanding for designing highly efficient QD white LEDs based on the scattering effect.

References

[1] E. F. Schubert, "Solid-state light sources getting smart," *Science*, vol. 308, no. 5726, pp. 1274–1278, May 2005.

[2] S. Pimputkar, J. S. Speck, S. P. DenBaars, and S. Nakamura, "Prospects for LED lighting," *Nature Photon.*, vol. 3, no. 4, pp. 180–182, Apr. 2009.

[3] S. Nakamura, T. Mukai, and M. Senoh, "Candela-class high-brightness InGaN/AlGaN double-heterostructure blue-light-emitting diodes," *Appl. Phys. Lett.*, vol. 64, no. 13, pp. 1687–1689, Mar. 1994.

[4] K. J. Chen *et al.*, "Effect of the thermal characteristics of phosphor for the conformal and remote structures in white light-emitting diodes," *IEEE Photon. J.*, vol. 5, no. 5, Oct. 2013, Art. no. 8200508.

[5] Z.-T. Li *et al.*, "Investigation of light-extraction mechanisms of multi-scale patterned arrays with rough morphology for GaN-based thin-film LEDs," *IEEE Access*, vol. 7, pp. 73890–73898, 2019.

[6] X. B. Zou, H. Liang, and K. M. Lau, "Light extraction enhancement from GaN-based thin-film LEDs grown on silicon after substrate removal using HNA solution," *Phys. Status Solidi C*, vol. 7, nos. 7–8, pp. 2171–2173, 2010.

[7] S. Ye, F. Xiao, Y. X. Pan, Y. Y. Ma, and Q. Y. Zhang, "Phosphors in phosphor-converted white light-emitting diodes: Recent advances in materials, techniques and properties," *Mater. Sci. Eng., R, Rep.*, vol. 71, no. 1, pp. 1–34, Dec. 2010.

[8] Z.-T. Li, Q.-H. Wang, Y. Tang, C. Li, X.-R. Ding, and Z.-H. He, "Light extraction improvement for LED COB devices by introducing a patterned leadframe substrate configuration," *IEEE Trans. Electron Devices*, vol. 60, no. 4, pp. 1397–1403, Apr. 2013.

[9] J. Li, Z. Li, Z. Li, Y. Tang, X. Ding, and B. Yu, "Improvement in optical performance and color uniformity by optimizing the remote phosphor caps geometry for chip-on-board light emitting diodes," *Solid-State Electron.*, vol. 126, pp. 36–45, Dec. 2016.

[10] Z. Li, Y. Tang, J. Li, C. Wu, X. Ding, and B. Yu, "High color uniformity of white light-emitting diodes using chip-scaled package," *IEEE Photon. Technol. Lett.*, vol. 30, no. 11, pp. 989–992, Jun. 1, 2018.

[11] R. Hu, X. Luo, and H. Zheng, "Hotspot location shift in the high-power phosphor-converted white light-emitting diode packages," *Jpn. J. Appl. Phys.*, vol. 51, no. 9S2, Sep. 2012, Art. no. 09MK05.

[12] Y. Tang *et al.*, "Improvement of optical and thermal properties for quantum dots WLEDs by controlling layer location," *IEEE Access*, vol. 7, pp. 77642–77648, 2019.

[13] Z.-T. Li *et al.*, "Study on the thermal and optical performance of quantum dot white light-emitting diodes using metal-based inverted packaging structure," *IEEE Trans. Electron Devices*, vol. 66, no. 7, pp. 3020–3027, Jul. 2019.

[14] S. Nizamoglu, G. Zengin, and H. V. Demir, "Color-converting combinations of nanocrystal emitters for warm-white light generation with high color rendering index," *Appl. Phys. Lett.*, vol. 92, no. 3, Jan. 2008, Art. no. 031102.

[15] Y. Jin and X. Gao, "Plasmonic fluorescent quantum dots," *Nature Nanotechnol.*, vol. 4, no. 9, pp. 571–576, Sep. 2009.

[16] Y. Tang, Z. Li, Z.-T. Li, J.-S. Li, S.-D. Yu, and L.-S. Rao, "Enhancement of luminous efficiency and uniformity of CCT for quantum dot-converted LEDs by incorporating with ZnO nanoparticles," *IEEE Trans. Electron Devices*, vol. 65, no. 1, pp. 158–164, Jan. 2018.

[17] Z. Li *et al.*, "Highly efficient and Water-Stable lead halide perovskite quantum dots using superhydrophobic aerogel inorganic matrix for white light-emitting diodes," *Adv. Mater. Technol.*, vol. 5, no. 2, Feb. 2020, Art. no. 1900941.

[18] M. Stanisavljevic, S. Krizkova, M. Vaculovicova, R. Kizek, and V. Adam, "Quantum dots-fluorescence resonance energy transfer-based nanosensors and their application," *Biosensors Bioelectron.*, vol. 74, pp. 562–574, Dec. 2015.

[19] J. Zhou, Y. Yang, and C.-Y. Zhang, "Toward biocompatible semiconductor quantum dots: From biosynthesis and bioconjugation to biomedical application," *Chem. Rev.*, vol. 115, no. 21, pp. 11669–11717, Nov. 2015.

[20] T.-H. Kim *et al.*, "Full-colour quantum dot displays fabricated by transfer printing," *Nature Photon.*, vol. 5, no. 3, pp. 176–182, Mar. 2011.

[21] E. Jang, S. Jun, H. Jang, J. Lim, B. Kim, and Y. Kim, "White-light-emitting diodes with quantum dot color converters for display backlights," *Adv. Mater.*, vol. 22, no. 28, pp. 3076–3080, 2010.

[22] X. Dai *et al.*, "Solution-processed, high-performance light-emitting diodes based on quantum dots," *Nature*, vol. 515, no. 7525, pp. 96–99, Oct. 2014.

[23] M.-H. Shin, H.-G. Hong, H.-J. Kim, and Y.-J. Kim, "Enhancement of optical extraction efficiency in white LED package with quantum dot phosphors and air-gap structure," *Appl. Phys. Express*, vol. 7, no. 5, May 2014, Art. no. 052101.

[24] K. Xu *et al.*, "Light emission from a poly-silicon device with carrier injection engineering," *Mater. Sci. Eng., B*, vol. 231, pp. 28–31, May 2018.

[25] J.-S. Li, Y. Tang, Z.-T. Li, X.-R. Ding, L.-S. Rao, and B.-H. Yu, "Effect of quantum dot scattering and absorption on the optical performance of white light-emitting diodes," *IEEE Trans. Electron Devices*, vol. 65, no. 7, pp. 2877–2884, Jul. 2018.

[26] B. Xie, R. Hu, X. Yu, B. Shang, Y. Ma, and X. Luo, "Effect of packaging method on performance of light-emitting diodes with quantum dot phosphor," *IEEE Photon. Technol. Lett.*, vol. 28, no. 10, pp. 1115–1118, May 15, 2016.

[27] B. Xie *et al.*, "Targeting cooling for quantum dots in white QDs-LEDs by hexagonal boron nitride platelets with electrostatic bonding," *Adv. Funct. Mater.*, vol. 28, no. 30, Jul. 2018, Art. no. 1801407.

[28] H. C. Chen *et al.*, "Improvement in uniformity of emission by ZrO_2 nano-particles for white LEDs," *Nanotechnol.*, vol. 23, no. 26, Jul. 2012, Art. no. 265201.

[29] H. Zheng, L. Li, X. Lei, X. Yu, S. Liu, and X. Luo, "Optical performance enhancement for chip-on-board packaging LEDs by adding TiO2/Silicone encapsulation layer," *IEEE Electron Device Lett.*, vol. 35, no. 10, pp. 1046–1048, Oct. 2014.

[30] T.-H. Kim, S. Jun, K.-S. Cho, B. L. Choi, and E. Jang, "Bright and stable quantum dots and their applications in full-color displays," *MRS Bull.*, vol. 38, no. 9, pp. 712–720, Sep. 2013.

[31] J.-S. Li, Y. Tang, Z.-T. Li, Z. Li, X.-R. Ding, and L.-S. Rao, "Investigation of the emission spectral properties of carbon dots in packaged LEDs using TiO2 nanoparticles," *IEEE J. Sel. Topics Quantum Electron.*, vol. 23, no. 5, pp. 1–7, Sep. 2017.

[32] J.-S. Li, Y. Tang, Z.-T. Li, W.-Q. Kang, X.-R. Ding, and B.-H. Yu, "Study on reabsorption properties of quantum dot color convertors for light-emitting diode packaging," *J. Electron. Packag.*, vol. 141, no. 4, Dec. 2019, Art. no. 041006.

[33] K.-J. Chen *et al.*, "White light emitting diodes with enhanced CCT uniformity and luminous flux using ZrO₂ nanoparticles," *Nanoscale*, vol. 6, no. 10, pp. 5378–5383, 2014.

[34] Jacques, S. L, Wang, and Lihong, "Monte Carlo modeling of light transport in tissues," in *Optical-Thermal Response of Laser-Irradiated Tissue*, 1995, pp. 73–100.

[35] J.-Q. Xi *et al.*, "Optical thin-film materials with low refractive index for broadband elimination of fresnel reflection," *Nature Photon.*, vol. 1, no. 3, pp. 176–179, Mar. 2007.

[36] A. H. M. Shahadat Hussain and B. J. Tatarchuk, "Adsorptive desulfurization of jet and diesel fuels using Ag/TiO$_x$-Al₂o₃ and Ag/TiO$_x$-SiO₂ adsorbents," *Fuel*, vol. 107, pp. 465–473, May 2013.

[37] G. Y. Kim *et al.*, "Order-of-magnitude, broadband-enhanced light emission from quantum dots assembled in multiscale phase-separated block copolymers," *Nano Lett.*, vol. 19, no. 10, pp. 6827–6838, Oct. 2019.

[38] K. Xu, "Silicon MOS optoelectronic micro-nano structure based on reverse-biased PN junction," *Phys. Status Solidi A*, vol. 216, no. 7, Apr. 2019, Art. no. 1800868.

[39] K. Yee, "Numerical solution of initial boundary value problems involving Maxwell's equations in isotropic media," *IEEE Trans. Antennas Propag.*, vol. 14, no. 3, pp. 302–307, May 1966.

[40] J.-S. Li, Y. Tang, Z.-T. Li, K. Cao, C.-M. Yan, and X.-R. Ding, "Full spectral optical modeling of quantum-dot-converted elements for light-emitting diodes considering reabsorption and reemission effect," *Nanotechnology*, vol. 29, no. 29, Jul. 2018, Art. no. 295707.

[41] J. Li, Y. Tang, Z. Li, X. Ding, D. Yuan, and B. Yu, "Study on scattering and absorption properties of quantum-dot-converted elements for light-emitting diodes using finite-difference time-domain method," *Materials*, vol. 10, no. 11, p. 1264, 2017.

[42] A. Pannipitiya, I. D. Rukhlenko, M. Premaratne, H. T. Hattori, and G. P. Agrawal, "Improved transmission model for metal-dielectric-metal plasmonic waveguides with stub structure," *Opt. Express*, vol. 18, no. 6, p. 6191, Mar. 2010.

[43] J. Li, Y. Tang, Z. Li, X. Ding, B. Yu, and L. Lin, "Largely enhancing luminous efficacy, color-conversion efficiency, and stability for quantum-dot white LEDs using the two-dimensional hexagonal pore structure of SBA-15 mesoporous particles," *ACS Appl. Mater. Interfaces*, vol. 11, no. 20, pp. 18808–18816, May 2019.